Scientia Iranica (2024) 31(19), 1740–1751

Sharif University of Technology
Scientia Iranica
Transactions A: Civil Engineering
https://scientiairanica.sharif.edu

Experimental study on the effect of high power ultrasonic on the mechanical properties of concrete

Saber Saffar[*,1]

Department of Acoustics and Sound Engineering, IRIB University, P.O. Box 1986916511, Tehran, Iran.

Received 8 September 2021; received in revised form 27 Noveber 2022; accepted 5 April 2023

KEYWORDS
Concrete density;
Concrete water absorption;
High power ultrasonic waves;
Frequency;
Compressive strength;
3D printer.

Abstract. High compressive strength concrete is desirable in the construction industry. The valuable effect of high-power ultrasonic in the manufacturing industries is the motivation of this research in the construction industry. For this purpose, high-power ultrasound was employed to increase the compressive strength of concrete. Also, the effect of these waves on the water absorption of concrete has been studied. Ultrasonic waves were tested in two modes, one independently and the other in combination with the conventional concrete compaction method. The results did not show a significant change in the improvement of mechanical properties of concrete when using ultrasonic waves independently. However, in combination with the conventional method, the effect of waves on improving mechanical properties was significant. In this way, the results showed a 12.5% reduction in water absorption for cubic samples and illustrate a 15.5% for cylindrical samples. Furthermore, the results showed that the use of ultrasonic waves as an auxiliary process in the conventional method of concrete compaction increases by 12.5% and 15% in the compressive strength of cubic and cylindrical specimens, respectively. The results showed that high-power ultrasonic waves have great potential to be added to 3D concrete printer accessories for further research.

1. Introduction

Recent research illustrates that the construction industry is gradually engaging robotic and automated systems, mostly in the university and development Step with very limited practical usage in the construction industry [1–4]. There is a potential for material waste reduction, fast production, and decreasing labor costs when 3D printing is employed in the construction industry [5–9]. A very important point in 3DCP is the lower strength of concrete. The strength of concrete is a key factor that should not be sacrificed in new technologies such as 3DCP. One way to reduce the porosity and water absorption in concrete is to properly compact the concrete [10]. One of the most important challenges to increase the quality of concrete is choosing the right methods for compacting fresh concrete [11]. In this regard, mechanical vibrators are the common methods for compaction. Furthermore, elimination of

1. *Present address: Amirkabir University of Technology (Tehran Polytechnic), Department of Petroleum Engineering, Tehran, Iran.*
*. *Corresponding author. Tel.: +98 21 77249832*
E-mail address: s.saffar@aut.ac.ir (S. Saffar)

To cite this article:
S. Saffar "Experimental study on the effect of high power ultrasonic on the mechanical properties of concrete", *Scientia Iranica* (2024), **31**(19), pp. 1740–1751
https://doi.org/10.24200/sci.2023.59025.6022

the vibration weaknesses such as physical and mental damage because of sound (noise) pollution is desirable for construction industries [12]. In this study, concrete quality improvement by using high power ultrasonic hammer as a new method in compaction of concrete is the novelty of the present study. Previous studies have shown that high-power ultrasonic waves are very effective in increasing the density and refinedness of material [13]. High-power ultrasonic waves are often used as an auxiliary technology in most common production methods [14,15]. Research shows that the use of ultrasonic waves can reduce internal structural friction due to the increase of internal kinetic energy. It is for this reason that in production processes such as machining, turning, welding, shaping, and compression the forces required for shaping are reduced. [16–19]. Increasing the density of powder in the powder metallurgy process before sintering is very similar to compacting fresh concrete. In this regard, Abedini, Abdullah, and Alizadeh showed that ultrasonic waves increase the density of the powder during sintering and ultimately improve the mechanical properties of the manufactured product [20]. Unlike high-power ultrasonic, which has not been used in the concrete industry, low-power ultrasonic has been used in this industry for a long time. Recently, ultrasonic waves have been used to study the properties of fresh concrete in 3D printers. At the time being, high-power ultrasound is employed to mix concrete in pre-processing treatment. The ultrasonic mixing of cement paste offers great advantages for precast moulding, dry cast, and concrete plants [21]. Micro silica is widely used in the concrete today, leading to higher compressive strength than water and chemical-resistant concrete. The use of micro-and nanosilica or nanotubes leads to improvements in the compressive strength of high-performance concrete. Ultrasonic is very effective for the wetting, mixing, and dispersing of nanomaterials in cement or concrete. New nanomaterials, such as nano-silica or nanotubes lead to further improvements in resistance and strength [22]. Novel techniques such as Power Ultrasound (PUS) are currently under consideration to improve the hydration of cementitious materials and to promote the effectiveness of replacing supplementary cementitious materials. In this regard, Ganjian et al. outlines the possible mechanisms involved in the effects of PUS as a method to promote cement hydration kinetics of Portland cement and binary blends [23]. In the field of concrete microstructure, studies have been performed on the effect of high-power ultrasonic waves on fresh concrete. Serelis et al. created a binder that was adapted for 3D printers and the developing process was analyzed in detail. According to their research, early setting time and strength are gained due to ettringite crystal growth. Their results showed that the final setting time of developed binders varied from 5 min up to more than 20 min. Density, flexural and compressive strengths were investigated and compared to ordinary Portland cement. Compressive strength of ~ 1 MPa at 20 min and ~ 50 MPa at 28 days can be expected of 3D concrete printed samples [24].

Utilize glass powder in ultra-high performance concrete. Their results revealed, that high-frequency ultrasonic dispersion can significantly increase the hydration degree of binder and the compressive strength up to 16% [25].

In a conclusion, based on the similarity of the behaviour of waves in material environments, it can be expected that the replacement of conventional vibrators with ultrasonic waves by coupling to the head of a 3 DCP directly as an accessory tool can reduce many of the weaknesses and problems such as detachment, waterlogging, porosity, etc. Also, another positive side effect is noise pollution reduction, since it is beyond the range of human hearing. Therefore, since the strength of the concrete prepared by the 3D printers is less than the conventional methods, the use of technologies that can increase the strength will be very useful and effective. In this study, concrete compaction strength has been investigated using high-power ultrasonic waves.

2. Specifications of materials and equipment

2.1. Concrete

2.1.1. Aggregates

The sand and gravel depot sampling was performed based on Standard No. 11267. The sand and gravel grading curves used in Figures 1 and 2 are presented. The sieves used in the gravel granulation test are the numbers 1/2″, 1″, 3/4″, 3/8″, and scores 4 and 8, and the sub-sieve tray and sieves used in the sand granulation test were 3/8″ and the scores of 4, 8, 16, 30, 50, and 100 were sub-sized, respectively.

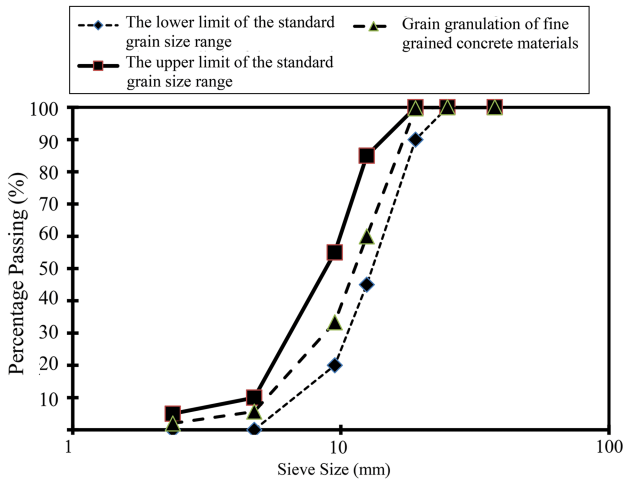

Figure 1. Fine-grained aggregate granulation curve used in concrete.

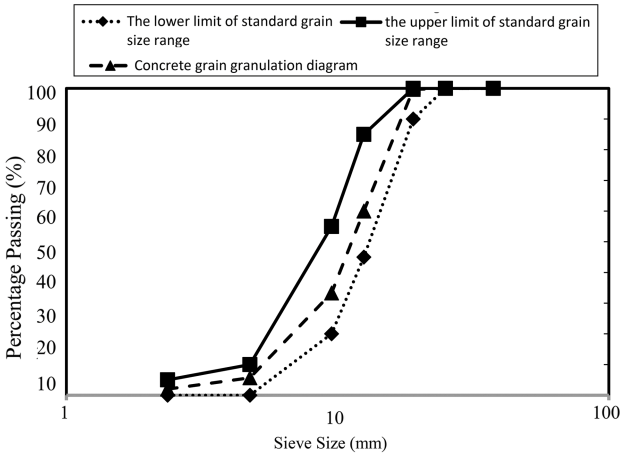

Figure 2. Coarse-grained aggregate granulation curve used in concrete.

As can be seen, the aggregates are within the standard range. It should be noted that the maximum size of coarse aggregate used in concrete is 12.5 mm and the fineness modulus is 3.42. Furthermore, the specific gravity was determined as 2449 kg/m^3 for coarse-grained and 2381 kg/m^3 for fine-grained materials in the saturated state with the dry surface.

2.1.2. Cement

The material specification of the cement is presented in Tables 1 and 2.

2.1.3. Sound power transmission to the load medium

In order to the maximum sound power transmission into the concrete environment, a suitable impedance matching between the transducer and the concrete should be done. to determine the appropriate acoustic impedances for matching the actuator source Piezo-Zirconate-Titanate (PZT) to the load medium (concrete), it is necessary to calculate the input mechanical impedance for each set of proposed matching layers. If the input mechanical impedance of the set of matching layers is close to the acoustic impedance of the PZT, then this set of matching layers is desirable, otherwise, it should be changed to another one. Hence, calculating of the input mechanical impedance of a bar is determined at first. Afterward, the input mechanical impedance of the multi-layers is derived. The input mechanical impedance for one degree of freedom system is [26]:

$$Z_m = R_m + jX_m, \qquad X_m = (\omega m - k/\omega), \tag{1}$$

where Z_m is the complex mechanical impedance (R_m and X_m are the real and imaginary parts, respectively). Also, ω, m, and k are the angular frequency, mass and stiffness, respectively. If this system is added to the end of an exciting simple bar (see Figure 3) the mechanical impedance at the interface Z_m can be calculated from Eq. (1), and the general solution of wave displacement and the boundary condition can be written as [26]:

$$u(x,t) = Ae^{j\left(\omega t - \overset{*}{k}x\right)} + Be^{j\left(\omega t + \overset{*}{k}x\right)}$$

$$\begin{cases} F(0,t) = -\rho s \overset{*}{c}{}^2 \frac{\partial u}{\partial x}\big|_{x=0} \\ \frac{\partial u}{\partial x}\big|_{x=L} = \frac{-Z_m}{\rho s \overset{*}{c}{}^2}\left(\frac{\partial u}{\partial t}\big|_{x=L}\right) \end{cases} \tag{2}$$

where A and B are the amplitude of incident and reflected waves, respectively, F is the force and s and $\overset{*}{c}$ are the cross section and complex speed of sound of layer. ρ is the density of the layer material.

Table 1. Chemical characteristics of cement used.

Subject	Na_2O	SO_3	MgO	CaO	Fe_2O_3	Al_2O_3	SiO_2	K_2O	C_3S	C_2S	C_3A	C_4AF
Permissible percentage	–	< 3	< 5	Nonlimited	< 6	< 6	> 20	Limited	–	–	$8 >$	–
Percentage in cement	0.37	1.89	3.22	62.28	3.86	4.76	20.79	0.86	52.59	20.03	7.16	10.87

Table 2. Physical characteristics of cement used.

Subject	Autoclave expansion (%)	Catch time (min)		Specific area (cm^2/gr)	Compressive strength (kg/cm^2)		
		Permitive	Final		3 days	7 days	28 days
Permissible percentage	0.8>	45<	360>	2800<	100<	175<	315<
Percentage in cement	0.21	153	212	3081	208	333	492

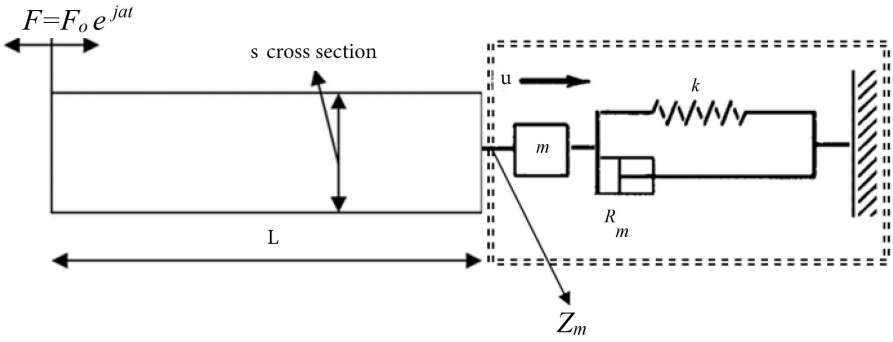

Figure 3. Damped oscillating system at the end of an excited cylinder layer.

by considering the boundary condition the solution can be written as:

$$\begin{aligned} u(x,t) =& (A_1 + jA_2)e^{j(\omega t-(k_1+jk_2)x)} \\ &+ (B_1 + jB_2)e^{j(\omega t+(k_1+jk_2)x)} \\ =& (A_1 + jA_2)e^{k_2 x}e^{j(\omega t-k_1 x)} + (B_1 + jB_2) \\ & e^{-k_2 x}e^{j(\omega t+k_1 x)} = A_1 e^{k_2 x}\cos(\omega t - k_1 x) \\ & - A_2 e^{k_2 x}\sin(\omega t - k_1 x) + B_1 e^{-k_2 x} \\ & \cos(\omega t + k_1 x) - B_2 e^{-k_2 x}\sin(\omega t + k_1 x) \\ & + j[A_1 e^{k_2 x}\sin(\omega t - k_1 x) + A_2 e^{k_2 x} \\ & \cos(\omega t - k_1 x) + B_1 e^{-k_2 x}\sin(\omega t + k_1 x) \\ & + B_2 e^{-k_2 x}\cos(\omega t + k_1 x)], \end{aligned} \tag{3}$$

$$A = -\frac{F_0 e^{j\overset{*}{k}L}}{2\omega s\rho\overset{*}{c}} \times \frac{1+\frac{Z_m}{\rho s\overset{*}{c}}}{\frac{Z_m}{j\rho s\overset{*}{c}}\cos\overset{*}{k}L + \sin\overset{*}{k}L} = A_1 + jA_2,$$

$$B = -\frac{F_0 e^{-j\overset{*}{k}L}}{2\omega s\rho\overset{*}{c}} \times \frac{1-\frac{Z_m}{\rho s\overset{*}{c}}}{\frac{Z_m}{j\rho s\overset{*}{c}}\cos\overset{*}{k}L + \sin\overset{*}{k}L} = B_1 + jB_2. \tag{4}$$

Particle velocity of wave is the time derivative of displacement (u).

$$\dot{u}(x,t) = \frac{F_0}{s\rho\overset{*}{c}} \frac{\cos\left[\overset{*}{k}(L-x)\right] + j\left(\frac{Z_m}{\rho s\overset{*}{c}}\right)\sin\left[\overset{*}{k}(L-x)\right]}{\left(\frac{Z_m}{\rho s\overset{*}{c}}\right)\cos\left[\overset{*}{k}(L-x)\right] + j\sin\left[\overset{*}{k}(L-x)\right]} e^{j\omega t}. \tag{5}$$

Therefore, the input mechanical impedance of the system can be given by Ref. [23] as follow:

$$Z_{\text{int}0} = \frac{F}{\dot{u}(0,t)} = s\rho\overset{*}{c}\frac{\left(\frac{Z_m}{\rho s\overset{*}{c}}\right) + j\tan\overset{*}{k}L}{1 + j\left(\frac{Z_m}{\rho s\overset{*}{c}}\right)\tan\overset{*}{k}L}. \tag{6}$$

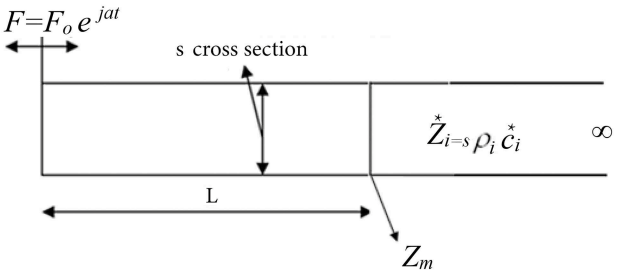

Figure 4. Excited cylinder layer connected along an infinity length cylinder layer.

If, $Z_m = \rho s\overset{*}{c}$, put in Eq. (6) then $Z_{\text{int}0} = \rho s\overset{*}{c}$. It means that the behaviour of the system is completely the same as the force vibration for an infinitive bar which is excited at one end. Indeed, the expressed equations can be used for the system shown in Figure 4.

2.1.4. Ultrasonic power

Based on the following simplified high power ultrasonic equation which shows the direct correlation of ultrasonic power with the amplitude of vibrations, the amplitude of vibrations can be changed by changing the power:

$$P(W) = ZS\omega^2 u^2, \tag{7}$$

where, P, Z, S, ω, and u are the ultrasonic power (Watt), the specific acoustic impedance (Rayl), transducer cross section, angular frequency (Hz), and vibration amplitude (m).

2.1.5. Ultrasonic transducer

To hold out the experiments, one ultrasonic transducer was designed and made to get the ultrasound energy needed for the experiments. To fabricate a transducer for pure one dimensional wave propagation, it's enough to model the vibration actuator for the PZT and matching and backing layer (s) within the Abaqus/ANSYS software to have a pure longitudinal resonance frequency are understood by changing the backing, PZT, and matching layer(s) thicknesses. As an example, Figure 5(a) illustrates an ultrasonic PZT actuator designed employing the Finite Element Method (FEM) after natural frequency

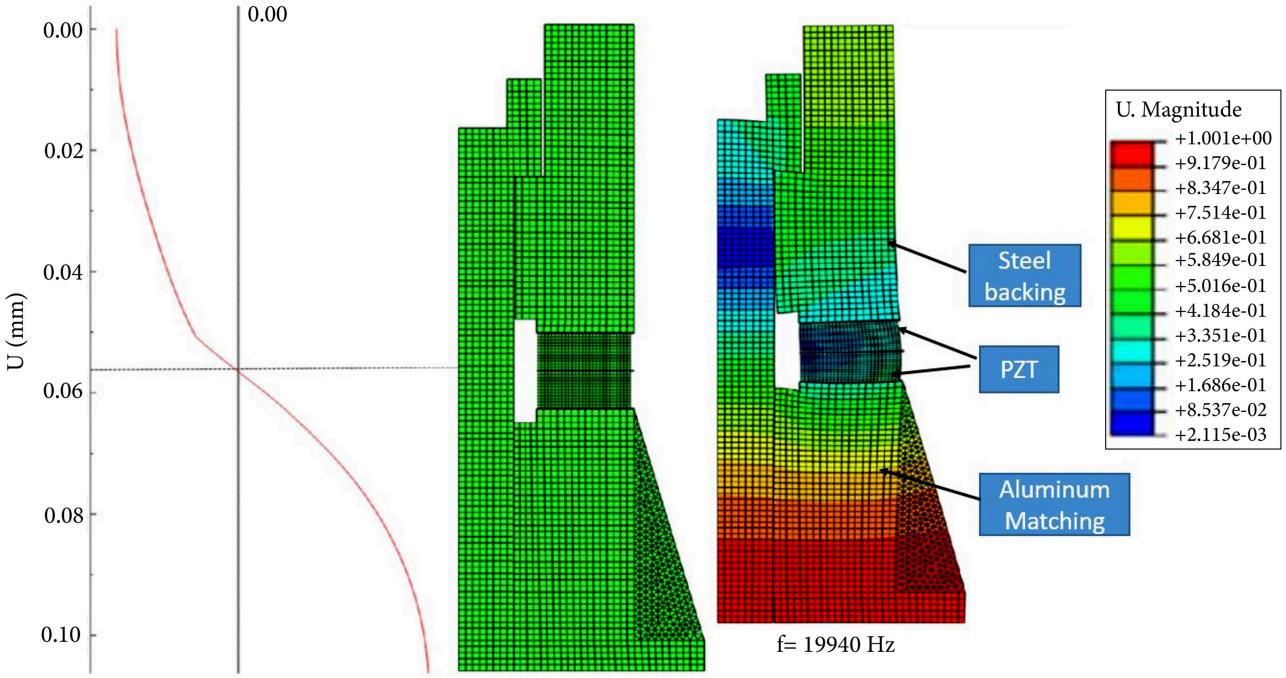

(a)

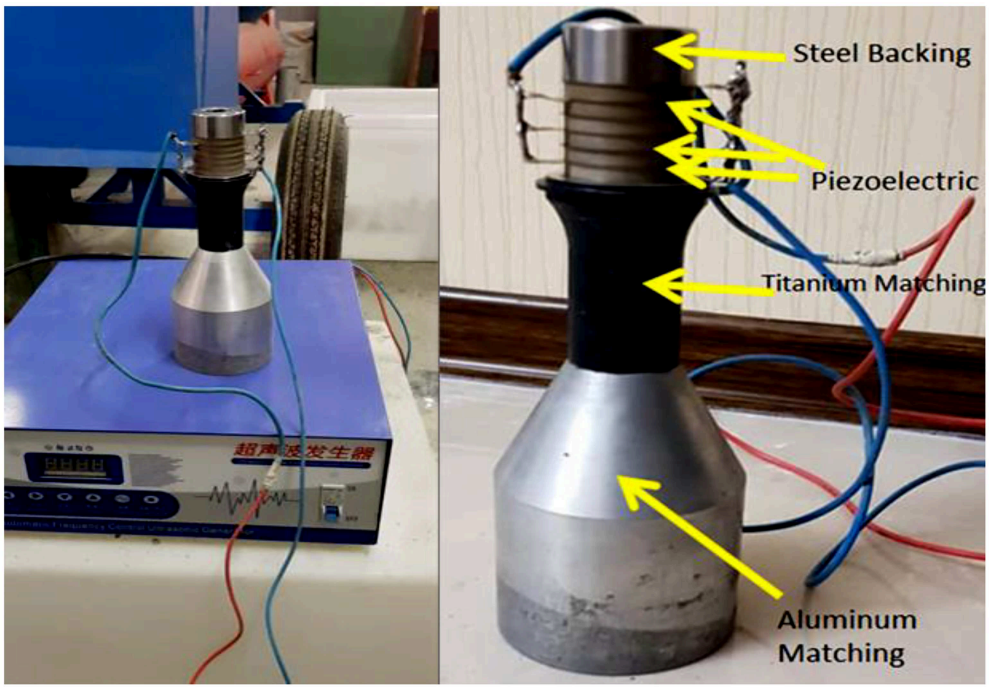

(b)

Figure 5. Transducer layers dimensions: (a) Calculated by ANSYS to have only plane wave; (b) Manufactured according to simulation.

analysis and determination of the matching layers to guaranty pure one-dimensional wave propagation. The ultrasonic actuator was manufactured consistently with the FEM recommendations, which is observed in Figure 5(b), and 20 kHz was selected because of the working frequency in all tests. The ultrasonic actuator consists of an aluminum matching, PZT actuators, and steel backing Figure 5(b) and Table 3, which are clamped together by applying 170 N-m torque to screw fasteners. The whole system must work at the resonance; Hence, to match the circuit to assist make sure that the transducer always works within the resonance situation, an electrical corresponding system is employed. The analytical estimations of the model

Table 3. Characteristics of a designed transducer.

Material	Role	Diameter (mm)			Thickness (mm)	Quantity
		Inner	Outer			
Lead Zirconate Titanium (PZT)	Vibration source	23	50		6	6
Titanium	First matching layer	22.6	Smaller	Bigger	90	1
			42	53		
Al 7075-T6	Second matching layer	22.6	Smaller	Bigger	110	1
			42	90		
Steel 304	Backing	22.6	51	–	50.6	1
Brass	Connection electrode for 2 PZT	22.8	51	–	0.5	3
High strength steel screw	Mechanical connecting parts	–	–	–	73.15	1

Table 4. Concrete characteristic used in research.

Soft modules	Ballast (kg)	Sand (kg)	Water /cement	Water (kg)	Cement (kg)	Maximum aggregate size (mm)	Concrete mix design
3.42	1060	642	0.6	243	405	12.5	B.S

Table 5. Type and number of specimens needed for test.

Specimen type	Test type	Specimen number				
		Standard method	Ultrasonic (30 s)	Ultrasonic (60 s)	Ultrasonic (90 s)	Standard+ ultrasonic (60 s)
Cylinder	Water absorption	3	–	3	–	3
	Compressive strength	3	–	3	–	3
Cubic	Water absorption	6	3	6	3	3
	Compressive strength	6	3	6	3	3

were compared, with experimental results. The used equipment is in Table 3. The ultrasonic generator provides vibration amplitudes at between zero and 20 micrometers.

3. Test method and requirement

3.1. Preparation of specimens

All samples were provided according to British Standard (B.S) which is presented in Table 4.

Based on B.S 1881 (British Standard), all tests have been run in two Steps, in the first step, 24 cubic specimens (with dimensions of $10 \times 10 \times 10$ cm^3) were produced, and in the second step, 36 specimens (18 cylindrical with dimensions of 10 cm in diameter and 20 cm in length and 18 cubic specimens) were prepared for compressive strength and water absorption tests (Table 5). For each test, 3 specimens (based on B.S 1881) are employed. Furthermore, a cylinder steel rod with an approximate diameter of 16 mm and length of 600 mm is used as the standard method. In this regard, concrete is poured into three layers in moulds and each layer is compacted by applying 25 strokes. After compaction of each layer, the outer surfaces of the mould are gently hammered to reduce the porosity. In specimens that are employed ultrasonic waves, each specimen is compacted in 3 layers by ultrasonic waves instead. In the compound method, in each specimen, firstly, the

Figure 6. Images of the steps of making cubic and cylindrical tests under standard.

Figure 7. Images of the steps of making cubic and cylindrical tests under the influence of ultrasonic waves.

compaction is done with the standard method and then the specimens are compressed using ultrasonic waves (Figures 6 and 7). The moulding process has been finished in 45 minutes due to having the same quality of concrete in all tests.

3.2. Production and processing of specimens

After compaction of concrete in the mould, the specimens are kept in the mould for 24 hours, the specimens hold at a temperature of $20 \pm 5°C$ and are protected from any shock, vibration, and loss of hydration water during this keeping time. Afterward, the specimens are pushed out from the mould and locate in the water bath at a temperature of $20 \pm 2°C$ until the test starts. Since the water absorption test should be performed when the specimens are at the age of 28 to 32 days, the specimens drying process should be started at the age of 24 days and the specimens should be held in the furnace with the temperature $105 \pm 5°C$ for 72 ± 2 hours.

3.3. Experimental test

3.3.1. Determination of the specimen's water absorption

The specimens are cooled in a desiccant container for 24 ± 0.5 hours after getting out of the furnace. Immediately after cooling, each specimen is weighed and recorded. The specimens are then immersed in a water tank for 30 ± 0.5 minutes. After this immersion time, the specimens are immediately picked out of the bath, and quickly dried with a clean and dry cloth. Each specimen is then carefully weighed and recorded. The water absorption of each specimen is calculated based on the weight gain due to immersion in water $(m - m_0)$ and the dry specimen mass by using the percentage of water absorbed: $[m - m_0/m] \times 100$ where, m and m_0 are the moisture and dry specimen mass, respectively.

3.3.2. Compressive strength test of specimens

The 28 life days specimens are candidates for compressive strength. For this purpose, the specimens are taken out of the water bath and directly placed in the test compressive machine. Afterward, the test samples are adjusted in the test compressive machine so that the applied load is perpendicular to the surface of the specimens. Also, the specimens were placed right in the center of the lower clamp. The constant loading rate was forced to the specimens without shock in the range of 0.6 ± 0.2 MPa.

4. Results

To find the optimal power, different powers are examined as a primary test to find the optimum ultrasonic

Table 6. The results of the water absorption tests of cubic specimens for tests in Step 1.

Average	Percentage of sample water absorption (%)			Samples weight (kg)			Condition	Densification method
	S3	S2	S1	S3	S2	S1		
5.683	5.665	5.679	5.707	2.030	2.025	2.015	Dry weight	Standard
				2.145	2.140	2.130	Wet weight	
6.015	6.000	6.030	6.015	2.000	1.990	1.995	Dry weight	Ultrasonic 30 s
				2.120	2.110	2.115	Wet weight	
5.617	5.568	5.673	5.611	2.040	2.035	2.030	Dry weight	Ultrasonic 60 s
				2.155	2.150	2.145	Wet weight	
5.665	5.615	5.675	5.665	2.035	2.030	2.020	Dry weight	Ultrasonic 90 s
				2.150	2.145	2.140	Wet weight	

power. Therefore, some primary tests have been carried out to determine the power required for the ultrasonic transducer. In this regard, several pre-tests performed at 200, 400, 600, 800, and 1000 watts. The results showed that capacities of less than 1000 watts did not have a significant effect. Therefore, the ultrasonic power was fixed at 1000 watts during the main tests. Also, the tests have been carried out in two steps:

Step 1: 24 cubic specimens used for both water absorption and compressive strength tests (12 for each test). In this step, we concentrate on the determination of the optimum time of ultrasonic wave transmission.

Step 2: 36 specimens (18 cubic and 18 cylindrical) for both water absorption and compressive strength tests. In this step, the effect of specimen shape in the optimum time of ultrasonic wave transmission was investigated.

4.1. Water absorption test

The results of the water absorption test of cubic specimens at the age of 28 days are presented in Tables 6 and 7 and Figure 8. As shown in Table 6, the minimum water absorption occurs at 60 s ultrasonic wave transmission continuously when ultrasonic is applied alone. The results illustrate that the ultrasonic has no significant effect in less time (the 30 s) rather than the standard method. Also, there is not much gain in higher time of ultrasonic wave transmission due to the waste of electrical power. The phenomenon, the name "cavitation" is the reason. when the time of ultrasonic increases, some of the water starts to evaporate. Therefore, as result, 60-second ultrasonic wave transmission is used for the rest of the tests (tests in Step 2). As shown in Table 7, the water absorption of concrete reduces by about 12.5% for cubic specimens when the ultrasonic is used as an

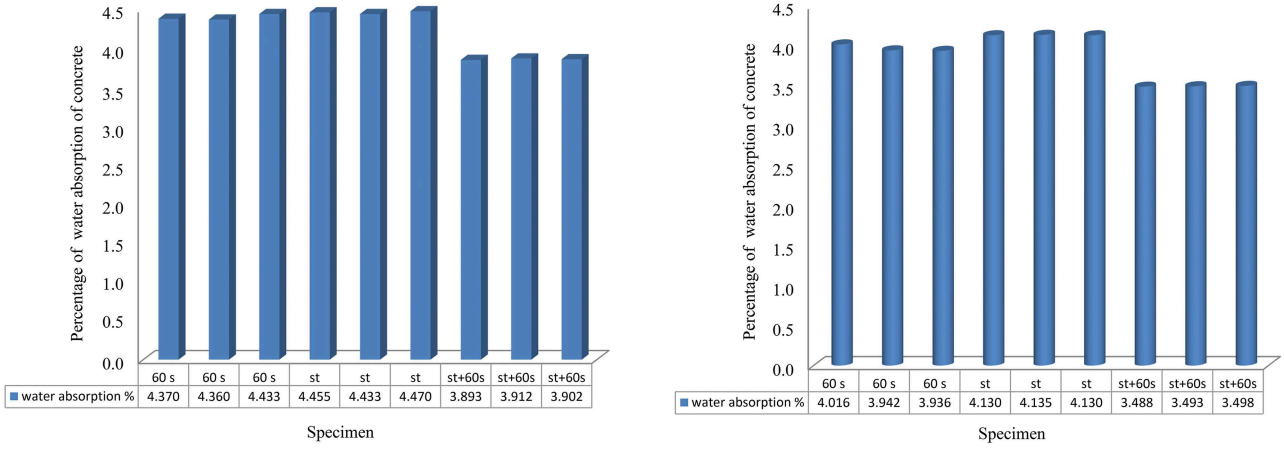

Figure 8. Comparison of water absorption test results of cubic and cylindrical specimens (step 2).

Table 7. The results of the water absorption test of both cubic and cylindrical specimens for tests in Step 2.

Average	Percentage of sample water absorption (%)			Samples weight (kg)			Condition	Densification method	Specimen type
	S3	S2	S1	S3	S2	S1			
4.453	4.470	4.433	4.455	2.025	2.030	2.020	Dry weight	Standard	Cubic
				2.115	2.120	2.110	Wet weight		
3.902	3.902	3.912	3.893	2.050	2.045	2.055	Dry weight	Ultrasonic 60 s	
				2.130	2.125	2.135	Wet weight		
4.354	4.333	4.360	4.370	2.035	2.045	2.035	Dry weight	Ultrasonic 60 s	
				2.130	2.130	2.125	Wet weight		
4.132	4.130	4.135	4.130	3.390	3.385	3.390	Dry weight	Standard	Cylindrical
				3.530	3.525	3.530	Wet weight		
3.493	3.498	3.493	3.488	3.430	3.435	3.440	Dry weight	Standars+ultrasonic 60 s	
				3.565	3.570	3.560	Wet weight		
3.964	3.936	3.942	4.016	3.410	3.395	3.420	Dry weight	Ultrasonic 60 s	
				3.485	3.455	3.540	Wet weight		

auxiliary process. Besides, in cylindrical specimens where the cross-sectional shape of the test mould and the transducer are the same, the reduction in water absorption is about 15.5%.

Ultrasonic waves convert the static friction coefficient to the dynamic friction coefficient, which is about 10 times less than the static friction coefficient. This phenomenon makes it easier for sand and cement particles to move on top of each other. Therefore, these results may be due to the fact that high-power ultrasonic waves have the ability to vibrate at very high frequencies and can help move particles inside fresh concrete in empty spaces. In fact, ultrasonic waves move inside fresh concrete, reducing friction between particles and helping them glide over each other to better fill voids. Waves can also help air bubbles escape into the concrete to make the concrete more compact, which ultimately reduces water absorption.

4.2. Compressive strength test

The results of the compressive strength test of cubic specimens at the age of 28 days are presented in Tables 8 and 9 for tests and Figure 9. As shown in Table 8, the maximum compressive strength reaches when the 60 s ultrasonic wave is applied continuously. The ultrasonic has no significant effect in less time (the 30 s) in comparison with the standard method. Also, the results show that ultrasound using is not economic due to the cavitation effect as explained in the previous step. Therefore, In the combined method (Ultrasonic+ standard), 60-second ultrasonic wave transmission is used for tests in Step 2. The results show that the compressive strength of concrete for cubic specimens increases by about 10% when ultrasonic is used as an auxiliary process. Also in cylindrical specimens where the cross-sectional shape of the used mould and the transducer are the same, the increase in compressive strength is about 14%.

As explained in the previous section, ultrasonic waves help reduce the structural friction of the concrete. This makes the particles inside the fresh concrete slide and moves more easily, filling in the gaps and

Table 8. The results of the compressive strength of the cubic specimens at the age of 28 days (in tests of Step 1).

Average (kg/cm^2)	Compressive strength of specimen (kg/cm^2)			Samples weight (kg)			Densification method
	S3	S2	S1	S3	S2	S1	
305	303	307	305	2.240	2.240	2.230	Standard
271.66	274	269	272	2.200	2.220	2190	Ultrasonic 30 s
311.33	309	312	313	2.250	2.250	2.245	Ultrasonic 60 s
307.66	306	309	308	2.240	2.245	2.235	Ultrasonic 90 s

Table 9. The results of the compressive strength of the cubic and cylindrical specimens at the age of 28 days (in tests of Step 2).

Average	Compressive strength of specimen(kg/cm^2)			Samples weight (kg)			Densification	Specimen
(kg/cm^2)	*S*3	*S*2	*S*1	*S*3	*S*2	*S*1	method	type
305	303	308	305	2.220	2.230	2.220	Standard	Cubic
336	333	336	339	2.230	2.240	2.240	Standard+ultrasonic 60 s	
312	310	312	314	2.230	2.235	2.230	Ultrasonic 60 s	
252	251	254	250	3.750	3.770	3.760	Standard	Cylindrical
288	288	287	290	3.780	3.790	3.800	Standard+ultrasonic 60 s	
259.66	260	258	261	3.760	3.785	3.785	Ultrasonic 60 s	

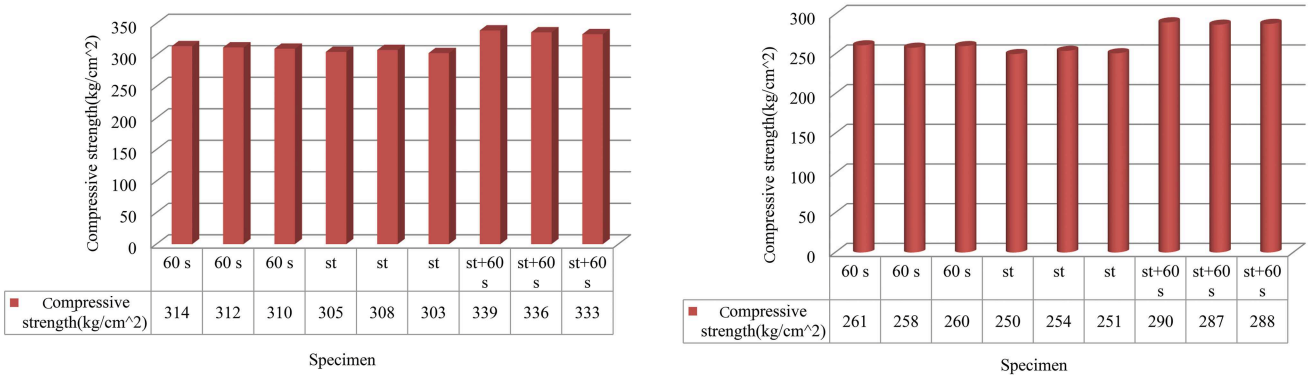

Figure 9. Comparison of compressive strength test results of cubic and cylindrical specimens (step 2).

helping to increase the density of the concrete. This increase in concrete density and decrease in voids helps to increase the compressive strength of concrete.

5. Conclusion

Increasing the quality of concrete and reducing costs is always very important for the construction industry. Concrete 3D printing has been introduced recently by some technology developers. Unfortunately, this method has not been able to find its place in the construction industry due to its low compressive strength. In this research, high- power ultrasonic waves have been employed to show that these waves can be useful and effective to increase the strength of concrete. High-power ultrasonic waves applied in the compaction of fresh concrete and their effect on compressive strength and water absorption of concrete were investigated and the shape of test moulds in ultrasound wave performance was examined as well. Different time intervals (30, 60 and 90 seconds) were used for transmitting ultrasonic waves, and it was shown that the optimal time to transmit ultrasonic waves to concrete was 60 seconds. Although the compressive strength increased lowly for a longer transmission time, it is not economical due to more energy consumption. Therefore, there is no economic interest in more than 60-second ultrasound use. In general, the results can be summarized as follows:

1. The maximum effect of high power ultrasonic occurs when the ultrasonic transducer shape (cross-section) and mould are the same;
2. The use of ultrasonic waves as an auxiliary process shows a 12.5% increase in water absorption tests for cubic specimens;
3. The use of ultrasonic waves as an auxiliary process shows a 15.5% increase in water absorption tests for cylindrical specimens;
4. The results showed that using of these waves (in optimal time) as an auxiliary process could increase the compressive strength by almost 10% for cubic specimens;
5. The results showed that using of these waves (in optimal time) as an auxiliary process could increase the compressive strength by almost 14% for cylindrical specimens.

Ultrasonic waves convert the static friction coefficient to the dynamic friction coefficient, which is about 10 times less than the static friction coefficient. This

phenomenon makes it simpler to move sand and cement particles. High-power ultrasonic waves are able to vibrate at very high frequencies and help particles move inside fresh concrete. Ultrasound waves can also help air bubbles escape into the concrete to make the concrete more compact, which ultimately reduces water absorption.

Preliminary results of this study show that in the next research, high-power ultrasonic waves can be used in the heads of 3DCP and the strength obtained from this combination of technology can be examined. This study aims to pave the way for research into the use of high-power ultrasonic waves in the 3DCP industry.

References

1. Cai, S., Ma, Z., and Skibniewski, M.J. "Construction automation and robotics for high-rise buildings over the past decades: A comprehensive review", *Advanced Engineering Informatics*, **42**(c), pp. 100–109 (2019). https://doi.org/10.1016/j.aei.2019.100989
2. Hofmann, E. and Rüsch, M. "Industry 4.0 and the current status as well as future prospects on logistics", *Comput. Ind.*, **89**, pp. 23–34 (2017). https://doi.org/10.1016/j.compind.2017.04.002
3. Davila Delgado, J.M., Oyedele, L., Ajayi, A., et al. "Robotics and automated systems in construction: Understanding industry-specific challenges for adoption", *J. Build. Eng.*, **26**, pp. 850–868 (2019). https://doi.org/10.1016/j.jobe.2019.100868
4. Bock, T. "The future of construction automation: Technological disruption and the upcoming ubiquity of robotics", *Autom. Constr.*, **59**, pp. 113–121 (2015). https://doi.org/10.1016/j.autcon.2015.07.022
5. Delgado Camacho, D., Clayton, P., O'Brien, W.J., et al. "Applications of additive manufacturing in the construction industry-A forward-looking review", *Autom. Constr.*, **89**, pp. 110–119 (2018). https://doi.org/10.22260/ISARC2017/0033
6. Rayna, T. and Striukova, L. "From rapid prototyping to home fabrication: How 3D printing is changing business model innovation", *Technol. Forecast. Soc. Chang.*, **102**, pp. 214–224 (2016). https://doi.org/10.1016/j.techfore.2015.07.023
7. Tay, Y.W.D., Panda, B., Paul, S.C., et al. "3D printing trends in building and construction industry: A review", *Virtual Phys. Prototyp.*, **12**, pp. 261–276 (2017). https://doi.org/10.1080/17452759.2017.1326724
8. Hager, I., Golonka, A., and Putanowicz, R. "3D printing of buildings and building components as the future of sustainable construction", *Procedia Eng.*, **151**, pp. 292–299 (2016). https://doi.org/10.1016/j.proeng.2016.07.357
9. Wu, P., Wang, J., and Wang, X. "A critical review of the use of 3-D printing in the construction industry", *Autom. Constr.*, **68**, pp. 21–31 (2016). https://doi.org/10.1016/j.autcon.2016.04.005
10. Zhang, J., Wang, J., Dong, S., et al. "A review of the current progress and application of 3D printed concrete", *Compos. Part A Appl. Sci. Manuf.*, **125**, pp. 345–353 (2019). DOI: 10.1016/j.compositesa.2019.105533
11. Zhang, J., Wang, J., Dong, S. et al. "A review of the current progress and application of 3D printed concrete", *Composites Part A: Applied Science and Manufacturing.*, **125**, pp. 350–359 (2019). DOI: 10.1016/j.compositesa.2019.105533
12. Howes, R., Hadi, S., and South, W. "Concrete strength reduction due to over compaction", *Construction and Building Materials.*, **197**, pp. 725–733 (2019). https://doi.org/10.1016/j.conbuildmat.2018.11.234
13. Abedini, R., Abdullah, A., and Alizadeh, Y. "Ultrasonic assisted hot metal powder compaction", *Ultrasonics Sonochemistry.*, **38**(C), pp. 704–710 (2016). https://doi.org/10.1016/j.ultsonch.2016.09.025
14. ASM Metals Handbook "Nondestractive Evaluation and Quality Control" (1989).
15. Siddiq, A. and El Sayed, T. "Ultrasonic-assisted manufacturing processes: Variational model and numerical simulations", *Ultrasonics*, **52**(4), pp. 521–529 (2012). https://doi.org/10.1016/j.ultras.2011.11.004
16. Kuo, K. and Tsao, C.-C. "Rotary ultrasonic-assisted milling of brittle materials", *Transactions of Nonferrous Metals Society of China*, **22**, pp. 793–800 (2012). DOI:10.1016/S1003-6326(12)61806-8
17. Nategh, M.J., Razavi, H., and Abdullah, A. "Analytical modeling and experimental investigation of ultrasonic-vibration assisted oblique turning, part I: Kinematics analysis", *International Journal of Mechanical Sciences*, **63**(1), pp. 1–11 (2012). https://doi.org/10.1016/j.ijmecsci.2012.04.007
18. Fartashvand, V., Abdullah, A., and Ali Sadough Vanini, S. "Effects of high power ultrasonic vibration on the cold compaction of titanium", *Ultrasonics Sonochemistry*, **36**(C), pp. 155–161 (2017). https://doi.org/10.1016/j.ultsonch.2016.11.017
19. Kumar, S., Wu, C.S., and Ding, W. "Application of ultrasonic vibrations in welding and metal processing: A status review", *Journal of Manufacturing Processes*, **26**(C), pp. 295–322 (2017). https://doi.org/10.1016/j.jmapro.2017.02.027
20. Abedini, R., Abdullah, A., and Alizadeh, Y. "Ultrasonic hot powder compaction of Ti-6Al-4V", *Ultrasonics Sonochemistry*, **37**(C), pp. 640–647 (2017). https://doi.org/10.1016/j.ultsonch.2017.02.012
21. Rößler, C. "Einfluss von power-ultraschall auf das fließ- und erstarrungsverhalten von zementsuspensionen", 17th *Int. Conf. Baustofftagung ibausil, Hrsg. Finger-Institut für Baustoffkunde*, Bauhaus-Universität Weimar, S., pp. 0259–0264 (2012).

22. Q. Liu, Z., Song, H., Cai, A., et al. "Effect of ultrasonic parameters on electrochemical chloride removal and rebar repassivation of reinforced concrete", *Journal of Materials*, **12**, pp. 277–281 (2019). https://doi.org/10.3390/ma12172774

23. Ganjian, E., Ehsani, A., Mason, T.J., et al. "Application of power ultrasound to cementitious materials: Advances, issues and perspectives", *Journal of Materials and Design*, **160**, pp. 503–513 (2018). https://doi.org/10.1016/j.matdes.2018.09.043

24. Vitoldas, V., Evaldas, S., and Vidas, K. "Effect of ultra-sonic activation on early hydration process in 3D concrete printing technology", *Construction and Building Materials*, **169**, pp. 354–363 (2018). DOI: 10.1016/J.CONBUILDMAT.2018.03.007

25. Evaldas, S., Vitoldas, V., Harald, H., et al. "Effect of ultra-sonic dispersion time on hydration process and microstructure development of ultra-high performance glass powder concrete", *Construction and Building Materials*, **298**, pp. 323–330 (2021). https://doi.org/10.1016/j.conbuildmat.2021.123856

26. Kinsler, L.E., *Fundamentals of Acoustics*, Ed., 4th., pp. 450–670, John Wiley and Sons Inc (2000).

Biography

Saber Saffar cooperating with IRIBU as a Professor Assistant in the Department of Acoustics and Audio Engineering. He is teaching advance vibration, fundamental of acoustic and architectural acoustic. He is also leading MSc students who interest in application of acoustics in engineering science. For instance, He is researching on the effect of acoustic waves on deactivating of hydatid cyst in human without surgery, these days. He is also cooperating with Amirkabir University (AUT) as a part time Adjunct Professor. He has gained valuable experiences leading MSc and BSc students of both universities since 2013.